ELSEVIER

Thermochimica Acta 359 (2000) 123–130

thermochimica acta

www.elsevier.com/locate/tca

Thermal behavior of the saccharinates of K^+, Na^+, Rb^+, Cs^+ and $NH_4{}^+$: structural inferences

Panče Naumov[a,*], Gligor Jovanovski[a], Sabina Abbrent[b], Lars-Erik Tergenius[b]

[a]Institute of Chemistry, Faculty of Sciences, Sv. Kiril i Metodij University, P.O. Box 162, MK-91001 Skopje, Macedonia
[b]Inorganic Chemistry, Ångström Laboratory, Uppsala University, P.O. Box 538, SE-75121 Uppsala, Sweden

Received 9 February 2000; received in revised form 10 April 2000; accepted 13 April 2000

Abstract

Four alkali saccharinates: $K_3(sac)_3{\cdot}2H_2O$ (KSac, 'sac' denotes saccharinato ion, $C_7H_4NO_3S^-$), triclinic $Na_3(sac)_3{\cdot}2H_2O$ (NaSac), $Rb_2(sac)_2{\cdot}H_2O$ (RbSac), $Cs(Hsac)(sac){\cdot}H_2O$ (CsSac)) and ammonium saccharinate (AmmSac) were synthesized and their thermal decompositions were investigated in the temperature interval 293–873 K by means of thermogravimetric methods (TG, DTG, DTA) in static atmosphere of helium and by DSC in a flow of nitrogen. The thermal and the infrared spectroscopic data of NaSac and AmmSac were correlated with the corresponding structural data, whereas data for KSac, RbSac and CsSac were used to make inferences about their crystal structures. Excluding the anhydrous AmmSac, all compounds were dehydrated prior to the decomposition of the deprotonated saccharinato species. The decomposition temperature of the saccharinato ion is about 130 K higher than the one of pure saccharin. There are two types of water molecules in molar ratio 2:1 in KSac, the overall structure being similar to but not identical with that of NaSac. Coordination properties rather than the hydrogen bonding are responsible for the stronger bonding of the water in the former salt. The existence of molecular saccharin in CsSac is confirmed. © 2000 Elsevier Science B.V. All rights reserved.

Keywords: Ammonium; Saccharinates; Structure; Thermal decomposition

1. Introduction

Owing to the suspected carcinogenic properties of saccharin as well as to the versatile coordination properties of its deprotonated form in saccharinato metal salts and complexes, much structural study has been devoted to the properties of saccharinates of various metals lately. Somewhat less extensive are the thermal data of saccharinates and these were often reported in brief as part of broader structural studies on various groups of saccharinates or their adducts with N-donor bases.

In continuation, a short review of the existing thermal data on saccharinates is presented. One of the earliest works in this area was the paper of Magri et al. [1] describing the thermal decomposition of $Co(sac)_2{\cdot}6H_2O$ and $Cu(sac)_2{\cdot}5H_2O$ and of their pyridine adducts $Co(py)(sac){\cdot}xH_2O$ (x=1,4) and $Cu(py)_2(sac)_2{\cdot}yH_2O$ (y=1, 2, 4) [1]. A subsequent paper [2] was devoted to the thermal properties of $Ni(sac)_2{\cdot}6H_2O$, $Zn(sac)_2{\cdot}6H_2O$, $Zn(py)_2(sac)_2{\cdot}H_2O$ and $Ni(py)_2(sac)_2{\cdot}8H_2O$. The thermal decompositions of the pyridine saccharinates of Ni(II), Cu(II), Zn(II) and Cd(II) in the temperature interval 303–623 K were later on reported by Romman et al. [3] and simulta-

---

[*] Corresponding author. Tel.: +389-91-11-70-55, ext. 527; fax: +389-91-22-68-65.
E-mail addresses: spance@iunona.pmf.ukim.edu.mk (P. Naumov), sabina.abbrent@kemi.uu.se (S. Abbrent)

PII: S0040-6031(00)00519-0

neously Ferrer et al. [4] published the decomposition of a oxovanadium(IV) complex described as a saccharin adduct. In a brief paper, Yugeng reported the thermal data of Cu(sac)$_2$·6H_2O and those of a mixed yttriumcopper ethanolate hydroxido complex [5]. The thermoanalytical curves of the anhydrous Zn(py)$_2$-(sac)$_2$ were discussed in connection with the corresponding crystal and molecular structure by Quinzani et al. [6]. Finally, a systematic reinvestigation of the thermal decompositions of the first transition row saccharinates of type [M(H_2O)$_4$(sac)$_2$]·2H_2O (M=Mn, Fe, Co, Ni, Cu, Zn) together with a kinetic analysis of the dehydration process was undertaken by Içbudak et al. [7]. Lately, this research group reported the thermal properties of the mixed hydrazine and ethylenediamine saccharinates of Co(II), Ni(II) and Cu(II) [8]. We [9] have recently investigated the thermal decompositions of the pyridine saccharinates of formulae [M(H_2O)$_4$(py)$_2$](sac)$_2$·4H_2O (M=Co and Ni) and [Cu(sac)$_2$(H_2O)(py)$_2$] and interpreted their decomposition pathways in sense of their crystal structures. In the same paper, a model for the decomposition of the saccharinato ligand in an oxidizing atmosphere was proposed.

Despite that the thermal data on saccharinates are somewhat less abundant than the structural ones, they can nevertheless be of great importance for structural characterization. One of the representative examples for the use of thermal data to solve structural dilemmas in the investigations of saccharinates is the thermal analysis of copper(II) 2,2′-bipyridine saccharinato complex. The decomposition pattern, namely, served as one of the key facts to choose the formula of a dihydrate for this compound [10] from two independent structural determinations [11,12].

In spite of their wide commercial use — primarily as artificial sweetening agents (especially saccharinates of Na and K), however, not much is known about the structures of saccharinates of the alkali metals. Up to date, the X-ray crystal structures only of NaSac (triclinic form) [13] and the mixed salt $K_2Na(sac)_3·H_2O$ [14] were reported. The crystal structure of AmmSac was published as well [15]. Within our broad study of saccharinates, we have undertaken a detailed and systematic structural study of the alkali saccharinates. Their vibrational spectroscopic characterization has been recently completed [16]. In the present paper, we report on their thermal decomposition (except for the lithium salt), in an attempt to predict additional structural data for these compounds of physiological interest.

1.1. Description of the structures of Na^+ and $NH_4{}^+$ saccharinates

Since more detailed discussion of the structures of NaSac and AmmSac is given elsewhere [13,15], only the points that are relevant for the present study will be briefly summed up here.

The structure of NaSac [13] is composed of sac$^-$ and Na^+ ions and water molecules. There are three structurally non-equivalent saccharinato ions as well as two crystallographically different water molecules in the unit cell. The corresponding formula is $Na_3(C_7H_4NO_3S)_3·2H_2O$. The structure of a pseudoalkali salt, ammonium saccharinate [15], is composed of saccharinato ions coordinated to ammonium cations. All saccharinato anions and ammonium ions are structurally equivalent. The compound is anhydrous and the corresponding formula is $NH_4C_7H_4NO_3S$.

2. Experimental

2.1. Synthesis of the compounds

Commercially available sodium saccharinate (very frequently and erroneously referred to as ‘saccharinum solubile’) was twice recrystallized from EtOH to obtain the triclinic NaSac. As stated by Jovanovski et al. [17], namely, another, monoclinic crystal form is obtained by recrystallization of sodium saccharinate from water solution. According to the spectroscopic evidence, this hydrate contains more than two molecules of water per formula unit and, therefore, cannot be considered a dihydrate. Owing to the partial dehydration during the preparation of the sample (as inspected via the infrared spectra), we were unable to record representative thermoanalytical curves of the monoclinic form of sodium saccharinate. The saccharinates of potassium (KSac), rubidium (RbSac) and cesium (CsSac) were obtained from the respective carbonates and saccharin dissolved in warm EtOH. Contrary to NaSac, recrystallization of KSac from water and EtOH, yielded the same compound.

AmmSac was prepared by mixing warm ethanolic solutions of ammonium carbonate and saccharin and slow evaporation of the mixture at room temperature (RT).

2.2. Analytical procedures

For the TG/DTG/DTA analyses a TG-DTA92 instrument (Setaram) and a static atmosphere of helium were used (Al_2O_3 crucible). The DSC measurements were performed with DSC20 oven (Mettler) connected to TA 400 temperature controller (Mettler), using Al containers (nitrogen, β=5 K min^{-1}, empty container served as reference). The temperature range for the heating experiments was from RT (ca. 293 K) to 873 K. The DSC curves for NaSac and AmmSac, in the temperature range from RT down to the boiling temperature of liquid nitrogen (LNT), were also recorded (β=5 K min^{-1}). Since our interest was mainly focused on the relative enthalpies, no caloric calibration was undertaken before each measurement. The temperatures were corrected against the melting temperature of pure saccharin (228.8–229.7°C). Data were evaluated using appropriate curve-fitting computer software. The FTIR spectra in the 4000–400 cm^{-1} frequency range were recorded from KBr pellets with System 2000 interferometer (Perkin-Elmer). A P/N 21525 (Graseby Specac) variable-temperature cell, equipped with KBr windows was used to record the low-temperature spectra. The elemental analyses were performed by standard methods.

3. Results and discussion

3.1. General discussion

The elemental analyses results as well as the thermal decomposition patterns of the compounds corresponded with the following stoichiometry: $K_3(sac)_3{\cdot}2H_2O$, $Na_3(sac)_3{\cdot}2H_2O$, $Rb_2(sac)_2{\cdot}H_2O$, $Cs(Hsac)(sac){\cdot}H_2O$ and $NH_4(sac)$. The formulae of NaSac and AmmSac were in agreement with the corresponding ones found by crystal structure determination [13,15]. It should be pointed out here that despite the identical formula found by this study for KSac and the triclinic NaSac, these two compounds have appreciably different X-ray powder diffraction patterns [17] and thus should not be isomorphous. No phase transitions were found for NaSac and AmmSac in the temperature interval from RT down to LNT (the DSC curves are not shown here).

3.1.1. Infrared spectra

Notable differences were observed among both RT and LNT infrared spectra of the compounds. Since that detailed discussion of their vibrational spectra can be found in [16], only some general points will be mentioned here. Except for AmmSac, prominent complex broad bands that originate from the water stretchings are present in the 3660–3100 cm^{-1} regions of the spectra of all compounds. However, the spectrum of CsSac is exceptional [18] for the absorption continuum centered around 2520 cm^{-1} that extends between 3200 and approximately 2200 cm^{-1}, with an Evans minimum around 2775 cm^{-1} (discussed below). The presence of this broad absorption band prescribed to NH stretching modes of saccharinato molecules [18] was recognized as clear evidence for the existence of molecular saccharin in the respective structure.

The stretching modes of the CO and SO_2 groups have been considered as the most valuable saccharinato bands for spectra–structure correlations. The carbonyl and sulfonyl stretching frequencies of the compounds investigated in the present study are listed in Table 1. A connection between the frequency shift to lower wavenumbers of the ν(CO) modes in the spectra of saccharinates from the saccharin ν(CO) frequency and the character of the respective metal–N(saccharinato) bonds has been established long ago [19,20]. The values of the shift, namely, ranged from about 30 cm^{-1} in the covalent mercury(II) saccharinates to more than about 80 cm^{-1} in purely ionic saccharinates (such as are NaSac and Mg saccharinate). The antisymmetric and the symmetric $\nu(SO_2)$ modes, moreover, have been regularly found lower than the corresponding saccharin values [21]. The ν(CO) frequency differences between studied saccharinates and saccharin (Table 1), therefore, are consistent with the existence of purely ionic saccharinato residues in their structures. The higher frequency of one of the ν(CO) bands as well as of one of the antisymmetric stretching SO_2 bands in case of CsSac

Table 1
LNT frequency data about the carbonyl and sulfonyl stretching in ammonium saccharinate (AmmSac) and the studied alkali saccharinates[a]

Parameter	Hsac	AmmSac	KSac	NaSac	RbSac	CsSac
$\tilde{\nu}[\nu(\mathrm{CO})]$	1725	1618 1578	1651	1635	1651 1624	1733 1621 1567
Average $\tilde{\nu}[\nu(\mathrm{CO})]$	1725	1598 (127)	1651 (74)[b]	1635 (90)	1637 (88)	1640 (85)
$\tilde{\nu}[\nu_{\mathrm{as}}(\mathrm{SO_2})]$	1335	1254 (81)	1257 (78)	1260 (75)	1271 (64)	1342 (−7) 1308 (27) 1258 (77)
$\tilde{\nu}[\nu_{\mathrm{s}}(\mathrm{SO_2})]$	1180	1147 (33)	1153 (27)	1150 (30)	1149 (31)	1177 (3) 1167 (13) 1149 (31)
Δ[c]	155	107	104	110	122	165 141 109
$\tilde{\nu}_{\mathrm{s}}/\tilde{\nu}_{\mathrm{as}}$[d]	0.884	0.915	0.917	0.913	0.904	0.877 0.892 0.913

[a] All values except for those in the last row are given in $\mathrm{cm^{-1}}$. The numbers in parentheses are the differences with the corresponding values of saccharin (Hsac is used for saccharin).

[b] Complex band.

[c] $\Delta=\tilde{\nu}[\nu_{\mathrm{as}}(\mathrm{SO_2})]-\tilde{\nu}[\nu_{\mathrm{s}}(\mathrm{SO_2})]$.

[d] $\tilde{\nu}_{\mathrm{s}}$ and $\tilde{\nu}_{\mathrm{as}}$ refer to $\tilde{\nu}[\nu_{\mathrm{s}}(\mathrm{SO_2})]$ and $\tilde{\nu}[\nu_{\mathrm{as}}(\mathrm{SO_2})]$, respectively.

confirms that this compound is adduct of molecular saccharin and thus comprises molecular saccharin in its structure. As can be concluded from Table 1, moreover, the frequencies of the ν(CO) bands of KSac and NaSac are appreciably different. Some differences are also observed between the frequencies of the ν(OH) and ν(OD) modes in the FTIR spectra of NaSac and KSac [17]. It goes along with the above-mentioned distinct structures of these two compounds, despite their analogous empirical formula.

3.2. Thermal decomposition

3.2.1. Dehydration of the compounds

With few exceptions, the decomposition pathways of NaSac and KSac are quite similar (Figs. 1 and 2), and therefore, will be simultaneously discussed. Their decomposition starts by partial dehydration slightly above RT (313 K by DTA and 323 K by DSC for NaSac, Fig. 1) with single well-defined DTG peaks. The dehydration onset of KSac (Fig. 2) is accompanied by an asymmetric endothermic DTA peak and, as estimated by DSC, starts at about 326 K. The similar temperatures of the initial dehydration of NaSac and KSac could be related to the similar strength of the bonding of the loosely bonded water molecules in the corresponding structures. However, the positions of the peaks (338 K for NaSac; 347 K for KSac by DSC) as well as the values of the integrated molar heats (68 kJ $\mathrm{mol^{-1}}$ for NaSac and 102 kJ $\mathrm{mol^{-1}}$ for KSac) corresponding to this process, imply that water molecules in the structure of KSac are more strongly bonded than those in NaSac. Although the view of the ν(OH) stretching region in their spectra is somewhat different [17], the bands appear in the same frequency range. It implies similar strength of hydrogen bonding of the water in these salts. Having all this in mind, it can be concluded that eventual differences in the coordination-bond strength would be one of the favorable factors to account for the above difference in the molar heats. The slight asymmetry of shapes of the DTA and DSC peaks imply that this step might be complex and that, after the initial water release,

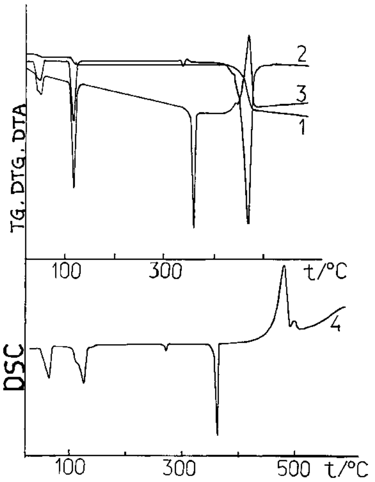

Fig. 1. Thermoanalytical curves of $Na_3(sac)_3{\cdot}2H_2O$ (1-TG, 2-DTG, 3-DTA, 4-DSC).

some structural disparity among the remaining water molecules might appear. Calculation of the respective mass losses clearly revealed that during this decomposition step of both compounds only one-third of the crystal water present leaves the samples. The initial step of dehydration, therefore, can be represented as

$$M_3(sac)_3 \cdot 2H_2O \rightarrow M_3(sac)_3 \cdot \tfrac{4}{3}H_2O + \tfrac{2}{3}H_2O$$
$$M = Na, K$$

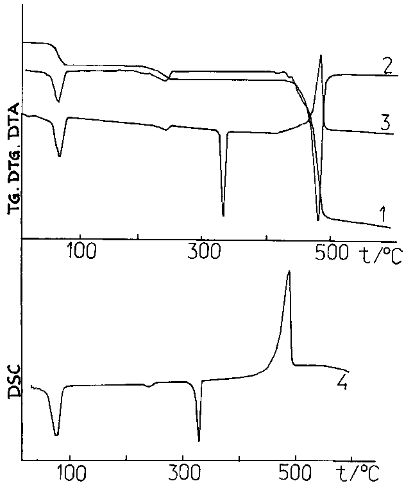

Fig. 2. Thermoanalytical curves of $K_3(sac)_3{\cdot}2H_2O$ (1-TG, 2-DTG, 3-DTA, 4-DSC).

The resulting partially dehydrated salts are stable up to 377 K (DTA)/387 K (DSC) and 489 K (DTA)/500 K (DSC) for NaSac and KSac, respectively, and afterwards are completely dehydrated. The significant difference between the temperatures of total dehydration during the second step is an indication that the difference in bonding strength of the remaining water in the two compounds is even greater. According to the nearly ideal agreement between calculated and experimentally observed mass loss ratios, the second dehydration step of both compounds can be represented as

$$M_3(sac)_3 \cdot \tfrac{4}{3}H_2O \rightarrow M_3(sac)_3 + \tfrac{4}{3}H_2O \quad M = Na, K$$

Nevertheless, the energetic profiles as well as the positions of this second dehydration step of NaSac and KSac are clearly different (Figs. 1 and 2). Namely, sharp and strong endothermic DTA (389 K) and DSC (401 K, 85 kJ mol^{-1}) peaks correspond to NaSac, whereas only a slight endothermic effect accompanies this process in the case of KSac (DTA peak at 513 K, DSC peak at 515 K, 5 kJ mol^{-1}). The structure of $Na_3(sac)_3{\cdot}4/3H_2O$ thus seems to be thermally less stable, but energetically more favorable than that of $K_3(sac)_3{\cdot}4/3H_2O$. This is supported by the difference in the temperatures and the specific heats of reaction corresponding to this step. The weak endothermic effect at 535 K present in the case of NaSac (DSC curve, Fig. 1) is probably due to some phase transition corresponding to minor structural changes, and therefore, requires rather small energy change (6 kJ mol^{-1}). The residues melt afterwards, which is demonstrated by sharp endothermic peaks (633 and 636 K for the DTA and DSC curves of NaSac, respectively, in Fig. 1; 605 and 601 K for the DTA and DSC curves of KSac, respectively, in Fig. 2) and are stable up to about 673 K (NaSac) and 693 K (KSac).

RbSac is far more stable than both NaSac and KSac and, except for the slightly endothermic effect observed on the DTA curve at about 443 K does not seem to undergo any structural change up to 463 K (Fig. 3). At this temperature the dehydration of the compound starts. Only one, apparently complex endothermic DTA peak (473 K) corresponds to this process, but two overlapping peaks (473 and 696 K, corresponding to 25 and 53 kJ mol^{-1}, respectively),

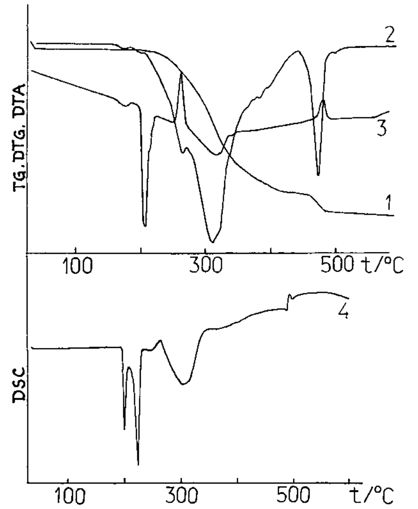

Fig. 3. Thermoanalytical curves of $Rb_2(sac)_2{\cdot}H_2O$ (1-TG, 2-DTG, 3-DTA, 4-DSC).

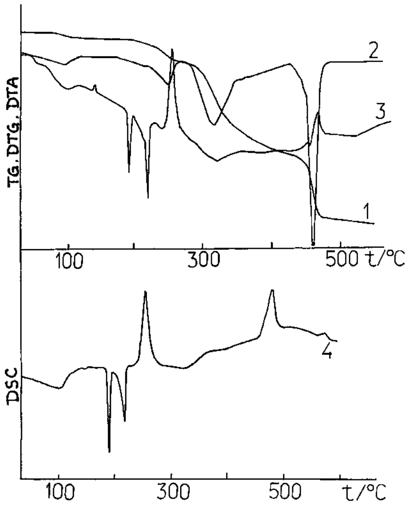

Fig. 4. Thermoanalytical curves of $Cs(Hsac)(sac){\cdot}H_2O$ (1-TG, 2-DTG, 3-DTA, 4-DSC).

can be inspected from the DSC curve. The dehydration of RbSac thus is a two-step process, but all the water molecules are probably structurally equivalent. The dehydration is followed by immediate decomposition of the dehydrated salt (Fig. 3). The higher initial temperature of dehydration of RbSac than both KSac and NaSac is in correspondence with the appreciable higher stability noted during handling of this compound.

The decomposition of CsSac (Fig. 4) starts with partial dehydration, yielding $Cs(Hsac)(sac){\cdot}0.5H_2O$. Since at the present heating rates of both DTA and DSC peaks diffuse, precise estimation of the initial dehydration temperature from the thermoanalytical curves was troublesome. The maximum of the DTA peak correspoding to this process is at 361 K (368 K from the DSC curve; specific energy change: 28 kJ mol^{-1}). The solid product ($Cs(Hsac)(sac){\cdot}0.5H_2O$) can be formally considered as a 'solid mixture' of $Cs(sac){\cdot}0.5H_2O$ and saccharin. Afterwards, the hemihydrate melts (462 K from the DTA and DSC curves; 15 kJ mol^{-1}) and undergoes complete dehydration, corresponding to the sharp peaks at 487 K (DTA) and 490 K (DSC; 22 kJ mol^{-1}). The residue is unstable and undergoes immediate decomposition. According to the above discussion, the dehydration of CsSac can be represented by the following equations:

$$\mathrm{Cs(Hsac)(sac)\cdot H_2O \rightarrow Cs(Hsac)(sac)\cdot \tfrac{1}{2}H_2O + \tfrac{1}{2}H_2O}$$

$$\mathrm{Cs(Hsac)(sac)\cdot \tfrac{1}{2}H_2O \rightarrow Cs(Hsac)(sac) + \tfrac{1}{2}H_2O}$$

3.2.2. Decompositions of the anhydrous saccharinates

According to the similarities of their decomposition pathways, dehydrated alkali saccharinates and AmmSac can be classified into three groups. The first group includes the dehydrated residues of NaSac and KSac, whereas the second group includes RbSac and CsSac. The decomposition pathway of AmmSac is different from those of the previous compounds and will be considered separately.

Anhydrous NaSac and KSac decompose in a similar manner, which is one more indication for the similarity between the structures of the respective starting compounds. The residues are stable over a relatively large temperature interval (Figs. 1 and 2). The decomposition of the sac ions starts at approximately 690 K, which is an about 130 K higher than the decomposition temperature of saccharin itself. Dehydrated NaSac and KSac undergo one-step, appreciably exothermic decomposition. Single well-defined DTA peaks at 753 K (758 K by DSC) and 756 K (761 K by DSC) correspond to NaSac and KSac, respectively. During this step, partial decomposition of the saccharinato ions occurs. The observed mass loss ratios fit well with the calculated values for release of SO_2 molecules

$$M_3(C_7H_4NO_3S)_3 \rightarrow M_3(C_7H_4NO)_3 + 3SO_2$$

when M represents Na, the mass loss calculated is 29.43%, the mass loss observed is 29.5%; and when M denotes K, the mass loss calculated is 27.46%, the mass loss observed is 27.7%.

Dehydrated RbSac and CsSac exhibit complex decomposition patterns (Figs. 3 and 4), each consisting of three steps, the first two being highly overlapped in the case of RbSac. The first decomposition step of both compounds is exothermic and is being characterized by single sharp DTA peaks at 533 K for RbSac and 529 K for CsSac. An analogy with the thermal behaviour of previously discussed NaSac and KSac might imply that this step represents release of sulfur dioxide. Owing to the extensive overlap, however, no direct confirmation can be made by comparison of the observed and the calculated values for the corresponding mass losses. The organic residue afterwards decomposes, leaving the respective alkali carbonate as residue, which is supported by the expected value of the overall mass losses (calculated: 58.25%, observed: 61.25% for RbSac; calculated: 29.61%, observed: 29.41% for CsSac). Broad endothermic DTA peaks correspond to this process (589 K for RbSac, 599 K for CsSac). The carbonates afterwards decompose to give the respective oxides, accompanied by sharp defined endothermic peaks on the DTA (745 K for RbSac, 749 K for CsSac) as well as on the DSC curves (766 K for RbSac and 751 K for CsSac).

The decomposition of the anhydrous AmmSac starts at about 430 K (Fig. 5) by complete deammination. This process is accompanied by two DTA and three DSC sharp and overlapped endothermic peaks. Remaining molecular saccharin adopts immediate two-step decomposition. The decomposition starts at about 510 K, which is about 50 K lower than pure saccharin. This indicates that the structure of saccharin obtained after the removal of ammonia from AmmSac is not as compact as the one of pure saccharin itself. The residual saccharin is thus more easily decomposed than pure saccharin. In accordance with such assumptions, the maximum of the first endothermic DTA peak (553 K) is lower than the one of pure saccharin (610 K). Being broad and weaker, the appearance of the corresponding endothermic DTA and DSC peaks is apparently different from that of the preceding deammination peaks. The decomposition is over and the crucible is empty at about 675 K.

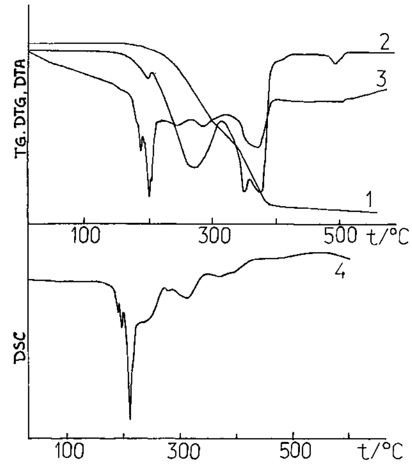

Fig. 5. Thermoanalytical curves of NH_4(sac) (1-TG, 2-DTG, 3-DTA, 4-DSC).

References

[1] A.D. Magri, G. D'Ascenzo, S. Nunziante Cesaro, E. Chiacchierini, Thermochim. Acta 36 (1980) 279.
[2] G. D'Ascenzo, R. Curini, A. Marino, A. Magri, E. Chiacchierini, Thermochim. Acta 59 (1982) 63.
[3] U.K.R. Romman, K.M.A. Malik, S.Z. Haider, J. Bangladesh Acad. Sci. 17 (1993) 165.
[4] E.G. Ferrer, S.B. Etcheverry, E.J. Baran, Monatsh. Chem. 124 (1993) 355.
[5] Z. Yugeng, Transit. Met. Chem. 19 (1994) 446.
[6] O.V. Quinzani, S. Tarulli, O.E. Piro, E.J. Baran, E.E. Castellano, Z. Naturforsch. 52b (1997) 183.
[7] H. Içbudak, V.T. Yilmaz, H. Ölmez, J. Thermal Anal. 53 (1998) 843.
[8] H. Içbudak, T.K. Yazicilar, V.T. Yilmaz, Thermochim. Acta 335 (1999) 93.
[9] P. Naumov, G. Jovanovski, V. Jordanovska, B. Boyanov, J. Serb. Chem. Soc. 64 (1999) 609.
[10] O. Grupče, G. Jovanovski, B. Šoptrajanov, A. Hergold-Brundić, Acta Crystallogr. 54c (1998) 890.
[11] A. Hergold Brundić, O. Grupče, G. Jovanovski, Acta Crystallogr. 47C (1991) 2659.

[12] J.-M. Li, W.-B. Lin, Y.-G. Zhang, S.-X. Liu, J.-L. Huang, Polyhedron 10 (1991) 403.

[13] G. Jovanovski, B. Kamenar, Cryst. Struct. Commun. 11 (1982) 247.

[14] K.M.A. Malik, S.Z. Haider, M.A. Hossain, Acta Crystallogr. C40 (1984) 1696.

[15] S.W. Ng, Acta Crystallogr. C54 (1998) 649.

[16] P. Naumov, G. Jovanovski, Spectrochim. Acta, A, 56/57 (2000) 1305.

[17] G. Jovanovski, O. Grupče, B. Šoptrajanov, J. Mol. Struct. 219 (1990) 61.

[18] P. Naumov, G. Jovanovski, Vibr. Spectrosc. 2000, in press.

[19] G. Jovanovski, B. Šoptrajanov, J. Mol. Struct. 174 (1988) 467.

[20] G. Jovanovski, B. Šoptrajanov, B. Kamenar, Bull. Chem. Technol. Macedonia 8 (1990) 47.

[21] G. Jovanovski, S. Tančeva, B. Šoptrajanov, Spectrosc. Lett. 28 (1995) 1095.